Stony Brook University
Academic Commons

SoMAS Research Data | School of Marine & Atmospheric Sciences

Spring 3-15-2019

Data for paper "Microbial generation of elemental mercury from dissolved methylmercury in seawater"

Cheng-Shiuan Lee
SUNY Stony Brook, cheng-shiuan.lee@stonybrook.edu

Nicholas S. Fisher
SUNY Stony Brook, nicholas.fisher@stonybrook.edu

Follow this and additional works at: https://commons.library.stonybrook.edu/somasdata

 Part of the Biogeochemistry Commons, and the Oceanography Commons

Recommended Citation

Lee, Cheng-Shiuan and Fisher, Nicholas S., "Data for paper "Microbial generation of elemental mercury from dissolved methylmercury in seawater"" (2019). *SoMAS Research Data*. 10.
https://commons.library.stonybrook.edu/somasdata/10

This Research Data is brought to you for free and open access by the School of Marine & Atmospheric Sciences at Academic Commons. It has been accepted for inclusion in SoMAS Research Data by an authorized administrator of Academic Commons. For more information, please contact mona.ramonetti@stonybrook.edu, hu.wang.2@stonybrook.edu.

LIMNOLOGY and OCEANOGRAPHY

ASLO

Limnol. Oceanogr. 64, 2019, 679–693
© 2018 Association for the Sciences of Limnology and Oceanography
doi: 10.1002/lno.11068

Microbial generation of elemental mercury from dissolved methylmercury in seawater

Cheng-Shiuan Lee ,* **Nicholas S. Fisher**
School of Marine and Atmospheric Sciences, Stony Brook University, Stony Brook, New York

Abstract

Elemental mercury (Hg^0) formation from other mercury species in seawater results from photoreduction and microbial activity, leading to possible evasion from seawater to overlying air. Microbial conversion of monomethylmercury (MeHg) to Hg^0 in seawater remains unquantified. A rapid radioassay method was developed using gamma-emitting ^{203}Hg as a tracer to evaluate Hg^0 production from Hg(II) and MeHg in the low pM range. Bacterioplankton assemblages in Atlantic surface seawater and Long Island Sound water were found to rapidly produce Hg^0, with production rate constants being directly related to bacterial biomass and independent of dissolved Hg(II) and MeHg concentrations. About 32% of Hg(II) and 19% of MeHg were converted to Hg^0 in 4 d in Atlantic surface seawater containing low-bacterial biomass, and in Long Island Sound water with higher bacterial biomass, 54% of Hg(II) and 8% of MeHg were transformed to Hg^0. Decreasing temperatures from 24°C to 4°C reduced Hg^0 production rates $cell^{-1}$ from Hg(II) 3.3 times as much as from a MeHg source. Because Hg^0 production rates were linearly related to microbial biomass and temperature, and microbial mercuric reductase was detected in our field samples, we inferred that microbial metabolic activities and enzymatic reactions primarily govern Hg^0 formation in subsurface waters where light penetration is diminished.

Elemental Hg (Hg^0) can be found at all depths in the ocean and is usually supersaturated in surface waters (Mason and Fitzgerald 1993), resulting in its subsequent evasion from the sea surface to the overlying air. Several studies have demonstrated the significance of Hg^0 evasion from the surface ocean (Fitzgerald et al. 1984; Kim and Fitzgerald 1986; Mason et al. 1994; Rolfhus and Fitzgerald 2001; Mason and Sheu 2002). The sea–air exchange of Hg^0 is rapid and is associated directly with Hg^0 concentrations in surface waters. Therefore, the transformation of other Hg species to Hg^0 is an important process in marine Hg cycling. In the mixed layer, Hg^0 can be produced by biological and/or photochemical reduction of reactive Hg(II) (Amyot et al. 1994, 1997; Rolfhus and Fitzgerald 2004), leading to decreased Hg(II) concentrations in the water column and therefore avoiding further methylation of Hg(II). Moreover, monomethylmercury (MeHg) can also be converted to Hg^0 through biotic and/or abiotic demethylation processes in soils and lakes (Oremland et al. 1991; Sellers et al. 1996). Both Hg(II) and MeHg are toxic, and the latter is bioaccumulative in aquatic organisms and can build up in aquatic food chains (Mason et al. 1996; Lawson and Mason 1998). Hence, there is interest in processes that influence mercury speciation in natural waters.

Hg^0 formation in the surface mixed layer can involve a variety of complex abiotic and biotic processes. Abiotic processes such as photochemical reduction of Hg(II) has been shown to produce Hg^0, where solar radiation (visible and ultraviolet), dissolved organic matter, and inorganic free radicals are considered key factors involved in the photochemical formation of Hg^0 from Hg(II) (Nriagu 1994; Amyot et al. 1997; Costa and Liss 1999, 2000; Vost et al. 2012). In addition, photodegradation of MeHg can also produce Hg^0 (Suda et al. 1993; Sellers et al. 1996).

Biologically mediated processes like microbial Hg(II) reduction and MeHg demethylation have also been shown to form Hg^0 (Robinson and Tuovinen 1984; Barkay et al. 1991, 2003). These processes can be attributable to prokaryotes possessing the Hg-resistant *mer* operon at a relatively high Hg exposure condition (Yu et al. 1996; Morel et al. 1998). For example, the microbial mercuric reductase enzyme, *merA* governs the conversion of dissolved Hg(II) to volatile Hg^0. Microorganisms with enzymes of Hg-resistance are widespread from diverse environments (Barkay et al. 1989; Osborn et al. 1997; Vetriani et al. 2005; Gionfriddo et al. 2016). Whether the transcription of the *mer* operon can be induced at natural Hg concentrations (pico- or femtomolar range) is not fully understood.

*Correspondence: cheng-shiuan.lee@stonybrook.edu

Additional Supporting Information may be found in the online version of this article.

Poulain et al. (2007) reported that *merA* genes were present and expressed by microbes from remote polar waters. However, some studies suggested Hg^0 formation can occur by other uncharacterized microbial processes (Oremland et al. 1991; Barkay et al. 2003; Kuss et al. 2015). Recent studies further suggest that methanotrophs may play a role in controlling Hg transformation such as MeHg degradation (Vorobev et al. 2013; Lu et al. 2017). Hg(II) reduction can also be carried out by eukaryotic phytoplankton (Ben-Bassat and Mayer 1977; Mason et al. 1995), but the mechanism of this pathway is not well understood or is often overlooked. Recent studies showed that phototrophic microorganisms (bacteria and algae) can use Hg(II) as an electron sink to maintain intracellular redox homeostasis, producing Hg^0 and therefore modifying the availability of Hg to methylation sites (Grégoire and Poulain 2014, 2016). Also, intracellular photochemical degradation and volatilization of Hg(II) and MeHg in a marine microalga was recently reported (Kritee et al. 2017). Overall, microorganisms, especially bacteria, play a fundamental role in Hg(II) reduction and MeHg degradation to form Hg^0.

In the surface mixed layer, the relative importance of abiotic (photochemical) and biotic (microbial) processes on Hg transformation remains uncertain. Over the past decade, mass-independent fractionation (MIF) and mass-dependent fractionation (MDF) of mercury isotopes have been developed to investigate photochemical reactions of Hg species in various environments (Bergquist and Blum 2007, 2009). The distinct MIF signature caused by photochemical processes allows determination of the degree of photoreduction of Hg(II) (Zheng and Hintelmann 2009) and photodegradation of MeHg in natural waters (Point et al. 2011; Tsui et al. 2013). Although microbial transformation of Hg (*mer* mediated) exhibits only the MDF signature, the Hg isotope ratios can still serve as a tool in determining the role of microbial Hg(II) reduction (Kritee et al. 2007, 2008) and MeHg degradation (Kritee et al. 2009) in the environment.

To further explore the roles that microbial activity play in Hg^0 product, here we demonstrate how marine bacterioplankton convert MeHg to Hg^0 at prevailing ocean temperatures. We focused on Hg^0 formation mediated by natural assemblages of marine microorganisms from Atlantic Ocean surface seawater collected off Southampton, NY and Long Island Sound surface water (LIW) collected off Stony Brook, NY exposed to picomolar Hg concentrations. Studies quantifying the kinetics of Hg^0 transformation from MeHg are few, and our study investigates the kinetics of Hg^0 formation from MeHg as well as Hg(II) mediated by natural occurring marine bacterioplankton. We developed a device to determine the kinetics of Hg^0 formation from either dissolved Hg(II) or MeHg and used ^{203}Hg as a gamma-emitting radiotracer of Hg^0 gas formation. We further investigated how temperature and microbial abundance and metabolic activity influence Hg^0 production in seawater.

Materials and methods

^{203}Hg preparation and $Me^{203}Hg$ synthesis

The gamma-emitting radioisotope, ^{203}Hg (half-life = 46.6 d), was used in this study to trace the transformation of Hg species between dissolved and gaseous phases. Previously, this isotope was used in experiments to quantify bioaccumulation and trophic transfer of mercury in marine plankton assemblages exposed to environmentally realistic mercury concentrations (Lee and Fisher 2016, 2017). A solution of $^{203}Hg(II)$ in 1 M HCl was obtained from Eckert and Ziegler Isotope Products (Valencia, California) with a specific activity of 185 GBq g^{-1} and was further converted to methyl-^{203}Hg ($Me^{203}Hg$) in the lab following established methods (Rouleau and Block 1997; Lee and Fisher 2016). In brief, $^{203}Hg(II)$ solution was mixed with methylcobalamin ($C_{63}H_{91}CoN_{13}O_{14}P$) and acetate buffer at pH 5. Allowing the reaction to proceed in the dark for 18–24 h, $Me^{203}Hg$ was formed spontaneously. Following extraction by dichloromethane (CH_2Cl_2) and purification processes, $Me^{203}Hg$ was redissolved in Milli-Q® water and was ready to use. The conversion yield (fraction of ^{203}Hg recovered as $Me^{203}Hg$) was 98% ± 2% (n = 3). Activities of ^{203}Hg and $Me^{203}Hg$ used in this study ranged from 0.019 kBq L^{-1} to 2.23 kBq L^{-1}, corresponding to concentrations of 1–100 pM of total (stable plus radioactive) Hg. Radiotracer ^{203}Hg can provide precise, rapid, and direct measurement of Hg^0 formation in seawater, avoiding lengthy analytical procedures and potential contamination.

Natural bacterioplankton assemblages

The natural microbial assemblages used in this study were collected from Southampton, NY (8 km offshore, Lat. 40.77°N, Long. 72.43°W, 35 psu) and Stony Brook, NY (Lat. 40.92°N, Long. 73.15°W, 30 psu). Southampton seawater (SSW, referring to Atlantic surface water) was collected from the upper 10 m and was coarsely filtered (~ 100 μm) 6 yr previously, stored at 4°C in the dark, and brought to room temperature (22°C) 2 d before experiments. LIW was freshly collected during high tide 1 d prior to experiments. Background concentrations of Hg(II) were ~5 pM, and MeHg was close to the detection limit (~5 fM) in these two waters, as determined using Tekran 2600 and 2700 mercury analyzers, respectively (Munson et al. 2014). Seawater used for experiments was filtered through sterile 1 μm polycarbonate membranes to remove all large particles including phytoplankton and zooplankton, leaving only bacterioplankton and similarly sized (or smaller) particles in the seawater. In general, SSW and LIW contain microbial densities of about 0.2–0.4 × 10^6 cells mL^{-1} and 4–5 × 10^6 cells mL^{-1}, respectively. We used $SSW_{1\mu m}$ and $LIW_{1\mu m}$ to indicate 1 μm-filtered seawater with bacteria, and SSW_{ctrl} and LIW_{ctrl} to represent experimental controls, sterile-filtered (0.2 μm) or autoclaved seawater (see below).

General approach

Experimental setup

Figure 1 shows a schematic depiction of the experimental apparatus used in this study. All the experiments were performed in 250 mL Pyrex® Erlenmeyer flasks with Teflon-lined screw caps (containing two holes drilled through the caps for an air inlet and outlet). Seawater (200 mL) with its naturally occurring bacteria was injected with microliter quantities of ^{203}Hg or Me^{203}Hg solutions (dissolved in 1 M HCl and Milli-Q® water, respectively) with no equilibration period, yielding concentrations ranging from 1 pM to 100 pM. Flasks were incubated at a constant temperature (24°C or 4°C) under a 14 : 10 h light/dark cycle provided by cool white fluorescent lamps. Seawater was continuously bubbled gently with particle-free and Hg-free air and the produced gaseous ^{203}Hg species was then collected in a Hg trap through the air outlet. The Hg trap was made of a quartz tube, glass wool, and gold-coated beads purchased from Brooks Rand Instruments (Seattle, Washington) (Fig. 1). Gold traps have been used previously to capture volatile mercury species (Fitzgerald and Gill 1979; Fitzgerald et al. 2007); the quantity of Hg released from these cultures was far less than the binding capacity of the gold traps. Radioactivity of ^{203}Hg in the Hg traps from each culture was directly determined with an LKB Wallac 1282 Compugamma NaI(Tl) gamma detector at 279 keV. All samples were counted with standards and decay-corrected. Propagated counting errors were < 5%. From measured activities on traps, the percentage of Hg species transformed to Hg^0 gas was calculated as:

$$\%Hg^0\ \text{evolved} = \frac{[\text{Bq}\ ^{203}\text{Hg}]_{\text{trap}}}{[\text{Bq}\ ^{203}\text{Hg}]_{\text{added}}}$$

$[^{203}\text{Hg}]_{\text{added}}$ was measured at the beginning of the experiment (t = 0) to determine variation in added amounts. Radioactivity was converted to molar concentrations of Hg using the specific activity of the isotope at the time of measurement. The rate of Hg^0 formation attributed to microbial activity was calculated as:

$$\frac{[Hg^0\text{evolved}]_{\text{bacteria}} - [Hg^0\text{evolved}]_{\text{control}}}{[\text{Hg(II) or MeHg}]_{\text{dissolved}} \times \text{Time}}$$

Assuming microbial Hg(II) reduction and MeHg demethylation as irreversible pseudo-first order kinetics, the following equations apply:

$$\frac{d[\text{Hg(II) or MeHg}]_{\text{dissolved}}}{dt} = -k_r[\text{Hg(II) or MeHg}]_{\text{dissolved}} = \frac{d[Hg^0]_{\text{evolved}}}{dt}$$

where k_r is the pseudo-first order rate constant for gross reactions under the experimental conditions. Reversible reactions such as Hg^0 oxidation and Hg(II) methylation were neglected because with the continuous purging used in our experiments the Hg^0 concentrations would be negligible and these reactions would be unlikely to occur.

Of the various Hg species, the Henry's law coefficients of Hg^0 and dimethylmercury (DMHg) indicate they are highly volatile and could volatilize from the dissolved phase at ambient temperatures. Recent studies have shown the potential abiotic pathways of DMHg formation from MeHg mediated by reduced sulfur groups on mineral or organic surfaces (Jonsson et al. 2016), and in sulfidic aqueous solutions (Kanzler et al. 2018). To verify whether DMHg was produced in our experiments as well as distinguish Hg^0 from DMHg in the gas traps, we used another Hg trap, Bond Elut ENV (Agilent Tech., Santa Clara, California), which contains styrene-divinylbenzene polymeric resins and effectively collects volatile organomercury compounds (Baya et al. 2013). In preliminary experiments, produced gaseous Hg was first passed through a Bond Elut trap followed by a gold trap without exceeding the reported breakthrough volume of the Bond Elut trap. We found very little Hg retained in the Bond Elut trap and > 95% of the Hg was collected in the gold trap. The Bond Elut trap can also collect a small fraction of Hg^0 (Baya et al. 2013). Thus, we concluded that Hg^0 was the dominant

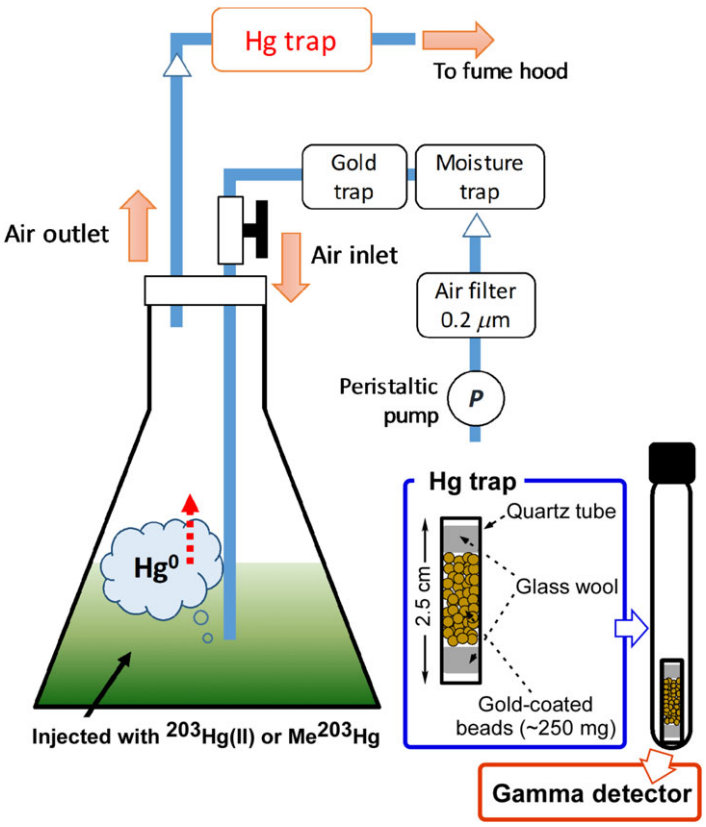

Fig. 1. Schematic layout of the incubation set-up and the Hg trap.

gaseous species produced in our study and Bond Elut traps were used in selected treatments to confirm no DMHg formation.

Short-term incubation experiments

We first performed a short term (1 d) incubation experiment to test the influence of Hg concentrations and microbial densities on Hg gas production. For experiments assessing different Hg concentrations, triplicate samples of 200 mL SSW with the same initial microbial density were injected with ^{203}Hg(II) or Me^{203}Hg at 1 pM, 10 pM, or 100 pM and then incubated for 24 h at 24°C under a 14 : 10 h light/dark cycle. For experiments assessing the influence of initial microbial density, duplicate samples of 200 mL SSW with varying initial microbial densities (by mixing with 0.2 μm filtered SSW) were prepared, with the addition of 10 pM of ^{203}Hg(II) or Me^{203}Hg in each treatment and incubated for 24 h at 24°C. After 24 h with continuous purging, Hg traps and 1 mL of unfiltered seawater were collected for radioanalysis, and the microbial densities were measured.

Long-term incubation experiments

A series of long-term (4 d) incubation experiments were carried out in order to evaluate the rates at which Hg gas evolved from each flask to overlying air. First, we determined the Hg gas production from three different types of controls, 0.2 μm sterile-filtered SSW (removing bacteria detectable with 4′,6-diamidino-2-phenylindole [DAPI] staining), autoclaved SSW (120°C for 30 min), and SSW with antibiotics (1% GE HyClone™ Penicillin-Streptomycin). Second, we examined how temperature (24°C vs. 4°C) and light (light vs. dark) influenced the Hg gas evolved from SSW. Third, we examined the Hg gas production in freshly collected LIW, as well as the difference between unfiltered LIW and 1 μm-filtered LIW.

Experimental procedures for long-term incubations were similar to those described in short-term experiments. Briefly, 200 mL seawater was injected with ^{203}Hg(II) or Me^{203}Hg at concentrations from 40 pM to 80 pM and incubated at either 4°C or 24°C with or without light. The Hg trap was collected and replaced with a new one at each sample time (4 h, 8 h, 12 h, 24 h, 36 h, 48 h, 72 h, and 96 h). In addition, 1 mL of unfiltered seawater was collected for microbial density determination at each sample time. Control treatments (seawater without bacteria) containing equivalent amounts of ^{203}Hg were performed simultaneously. To calculate the Hg mass balance ($[Hg]_{added} = [Hg]_{suspension} + [Hg]_{trap} + [Hg]_{flask\ wall}$, suspension = particulate + dissolved) in each flask, sorption of Hg(II) or MeHg onto culture flasks was examined by acid washing (1 M HCl) the flask walls at the end of the experiment. Across all experiments, the mass balance of Hg(II) and MeHg treatments were 94% ± 10% and 97% ± 2%, respectively.

Microbial density and microbial production

A modified DAPI staining method (Sherr et al. 2001) was used to count microbial densities. Microbial cell samples were fixed with 2% glutaraldehyde solution and were stored at 4°C. Prior to cell counts, cell samples were mixed with DAPI (1 μg mL^{-1}) and stained cells were then filtered onto a 0.2 μm black polycarbonate membrane at a vacuum pressure < 300 mmHg. Cell counts were obtained with the use of epifluorescence on an inverted microscope under ultraviolet light excitation. For each sample, the number of luminant dots (bacteria) in a whole grid for 10 randomly chosen fields over the membrane was counted and averaged. The average microbial density in each samples (cells mL^{-1}) was calculated from the equation:

$$\left[\frac{(\text{average cells per grid} - \text{background cells per grid}) \times \text{grids per filter}}{\text{volume of sample}}\right]$$

where background refers to 0.2 μm-filtered seawater subjected to the same DAPI-staining procedure. Microbial production measurements were performed as a parallel experiment to the Hg^0 formation experiments, using leucine incorporation method (Kirchman 1993). Radiolabeled L-[4,5-^{3}H]-leucine was purchased from PerkinElmer. In brief, 20 mL of unfiltered seawater was collected in an incubation vial at each time point (6 h, 12 h, 24 h, 48 h, 72 h, and 96 h), injected with ^{3}H-leucine to yield a concentration of 20 nM (corresponding to 24.8 kBq per vial) and incubated for 6 h. Incubation was terminated by adding trichloroacetic acid at a concentration of 5%. After heating for 20 min at 80°C, microbial cells were collected onto a 0.22 μm cellulose acetate filter at a vacuum pressure < 300 mmHg. The filter with cells was dissolved by adding ethyl acetate in a scintillation vial, mixed with Ultima Gold™ XR liquid scintillation cocktail. Beta radioactivity was determined using a PerkinElmer Tri-Carb® 2810 TR liquid scintillation analyzer. Because preliminary experiments indicated negligible microbial growth at 4°C, no microbial production measurements were conducted at this temperature.

Conventional polymerase chain reaction (PCR) analysis for mercuric reductase gene *merA*

Total DNA was extracted from seawater, using a PowerWater® Sterivex™ DNA isolation kit (MO BIO, Carlsbad, California). About 10 L of SSW and 2 L of LIW were filtered to collect enough DNA concentrations for analysis and *merA* was determined following the procedure of Poulain et al. (2015). PCR was performed using a Biometra® T3000 Thermocycler. PCR conditions consisted of a 10-min incubation at 95°C, followed by 35 cycles of 95°C for 30 s, 63°C for 15 s, 72°C for 30 s, and a final extension step at 72°C for 5 min. Final concentrations of the PCR mixture were 1× PCR buffer, 2.5 mM $MgCl_2$, 0.2 μM forward/reverse primers (merA2 F: CCTGCGTC AACGTCGGCTG, merA2 R: GCGATCAGGCAGCGGTCGAA), 0.2 mM dNTPs, and 1 U Taq Polymerase. Samples were analyzed with a positive control (*Pseudomonas aeruginosa*

containing the Hg resistance plasmid pVS1) (Lloyd et al. 2016), and a negative control (reagents only). Amplicons were separated by electrophoresis and visualized under ultraviolet light. Amplification of PCR product at the expected amplicon size (~ 300 bp) was used to determine the presence of *merA* in our samples.

Results

Effects of Hg concentrations and microbial biomass

The total percentage of Hg^0 gas evolved after 24 h as a function of dissolved Hg species concentrations and average microbial density is shown in Fig. 2. The $\%Hg^0$ evolved from each culture stayed almost constant across three different Hg concentrations (1–100 pM) at ~20% for Hg(II) treatments and ~5% for MeHg treatments (Fig. 2a). In these cultures, the initial microbial densities were 0.34–0.40 × 10^6 cells mL^{-1}, and the microbial densities at 24 h were 0.81–1.2 × 10^6 cells mL^{-1}. In separate experiments which used cultures with varying microbial cell densities and 10 pM of Hg(II) or MeHg, the % Hg^0 that evolved as a gas ranged from 6.2% to 31% in Hg(II) treatments and from 2.1% to 13% in MeHg treatments depending on the microbial abundance (Fig. 2b); Hg^0 released was positively correlated with microbial density. We performed each experiment twice and had consistent results. At the same microbial density, Hg^0 production was always higher from Hg(II) treatments than from MeHg treatments.

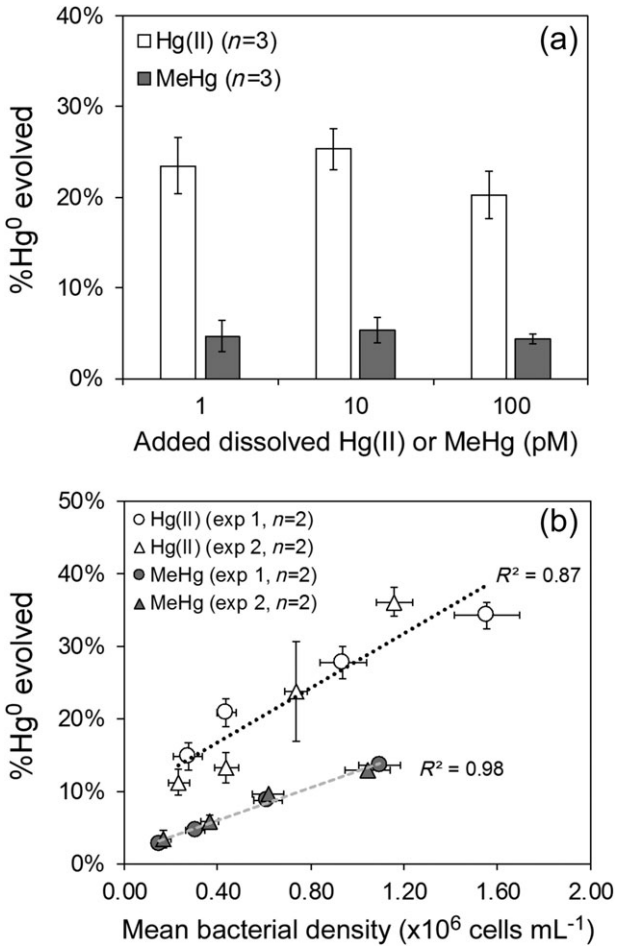

Fig. 2. Total percentage of $^{203}Hg^0$ evolved from $^{203}Hg(II)$- and $Me^{203}Hg$-treated SSW (1 μm-filtered) after 1-d incubation as a function of (**a**) dissolved Hg(II) or MeHg concentrations and (**b**) mean microbial cell density. Data points are the means from two or three replicate cultures with error bars of one standard deviation. Added concentrations of Hg(II) and MeHg were 10 pM in (**b**). Note that background concentrations of Hg(II) and MeHg in SSW were ~5 pM and ~5 fM, respectively.

Long-term incubations

Background Hg^0 production in SSW

The Hg^0 formation kinetics in three different control treatments are shown in Fig. 3. Generally, in Hg(II) treatments (Fig. 3a), 0.2 μm sterile-filtered SSW and autoclaved SSW had very similar patterns, rapid Hg^0 formation in the first 12 h followed by very slow formation, with an overall 5–9% of Hg^0 evolved. Controls with antibiotics showed almost no Hg^0 production in the first 24 h, but increased Hg^0 formation was observed after 36 h (Fig. 3a). In MeHg treatments (Fig. 3b), all

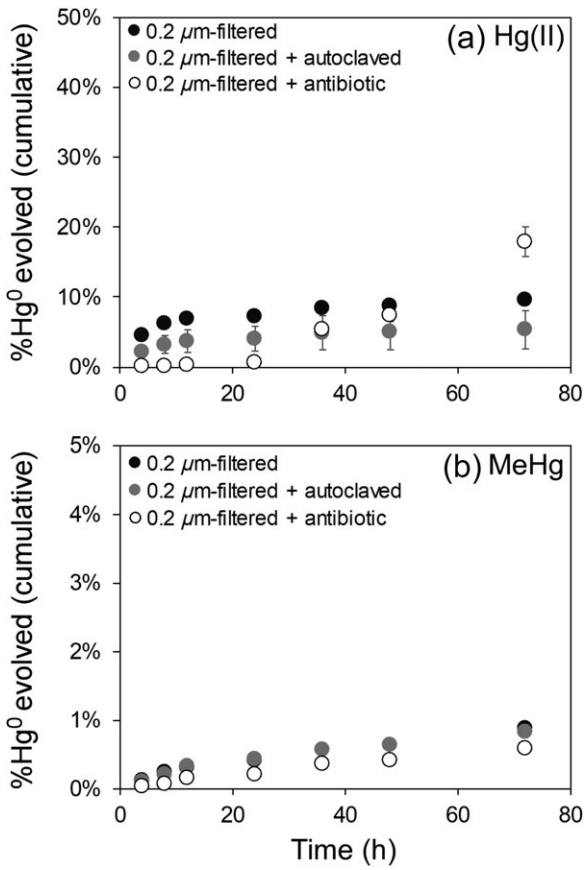

Fig. 3. Total percentage of Hg^0 evolved over time at 24°C from different controls (SSW without microbes) treated with (**a**) Hg(II) or (**b**) MeHg. Data points are the means from three replicate cultures with error bars of one standard deviation; error bars are often too small to see. Added concentrations of Hg(II) were 54 pM and of MeHg were 56 pM.

three types of controls showed very low Hg^0 formation over 72 h (overall < 1%), suggesting MeHg was very stable in seawater without bacteria. For all other experiments, we used 0.2 μm sterile-filtered seawater (SSW or LIW) for controls.

Effects of temperature and light

Figure 4a-c shows the Hg^0 evolved from Hg(II) and MeHg treatments in SSW over 96 h at two different temperatures, and their corresponding microbial cell densities. Rapid formation of Hg^0 in Hg(II)-treated SSW with bacteria within 24 h was observed (Fig. 4a). Total $\%Hg^0$ evolved was 32.6% ± 1.6% at 24°C after 96 h, but at 4°C it was only 8.0% ± 2.3%; this compares with total %Hg gas produced in controls of 7.6% ± 3.5% at 24°C and 5.6% ± 1.4% at 4°C. Thus, net production in microbial communities over 96 h was about 25% at 24°C and 2.5% at 4°C. Total Hg^0 evolved from MeHg-treated SSW with bacteria after 4 d was 18.9% ± 1.7% at 24°C and 10.2% ± 0.4% at 4°C, and both showed the same linear increasing patterns over time (Fig. 4b). Controls at two temperatures both showed very low Hg^0 production after 96 h (< 0.4%) and no microbial growth. Microbial growth was more pronounced at 24°C (more than one doubling after 96 h) than at 4°C, where scant growth occurred (Fig. 4c). The results of microbial production at 24°C are shown in Fig. 4d. The microbial production, as inferred from leucine uptake, increased over time, ranging from 0.09 μg-C L^{-1} h^{-1} to 0.35 μg-C L^{-1} h^{-1}. Normalized to microbial density, the estimated production rate ranged from 0.21 fg-C $cell^{-1}$ h^{-1} to 0.44 fg-C $cell^{-1}$ h^{-1}; normalized to bacterial carbon (20 fg-C $cell^{-1}$) (Lee and Fuhrman 1987), the microbial production increased at a rate of 1.1–2.2% d^{-1}. As the lower estimated value, which is the rate reflective of the initial production rate, closely matches the observed growth rate of the bacteria (increase in cell number d^{-1}) (Fig. 4c), it appears from the leucine incorporation rates that all the cells observed by DAPI were metabolically active.

For both Hg(II) and MeHg treatments, there was no significant difference in Hg^0 production between light and dark conditions (Fig. 5). Neither Hg^0 formation in controls nor microbial growth was affected by light (data not shown).

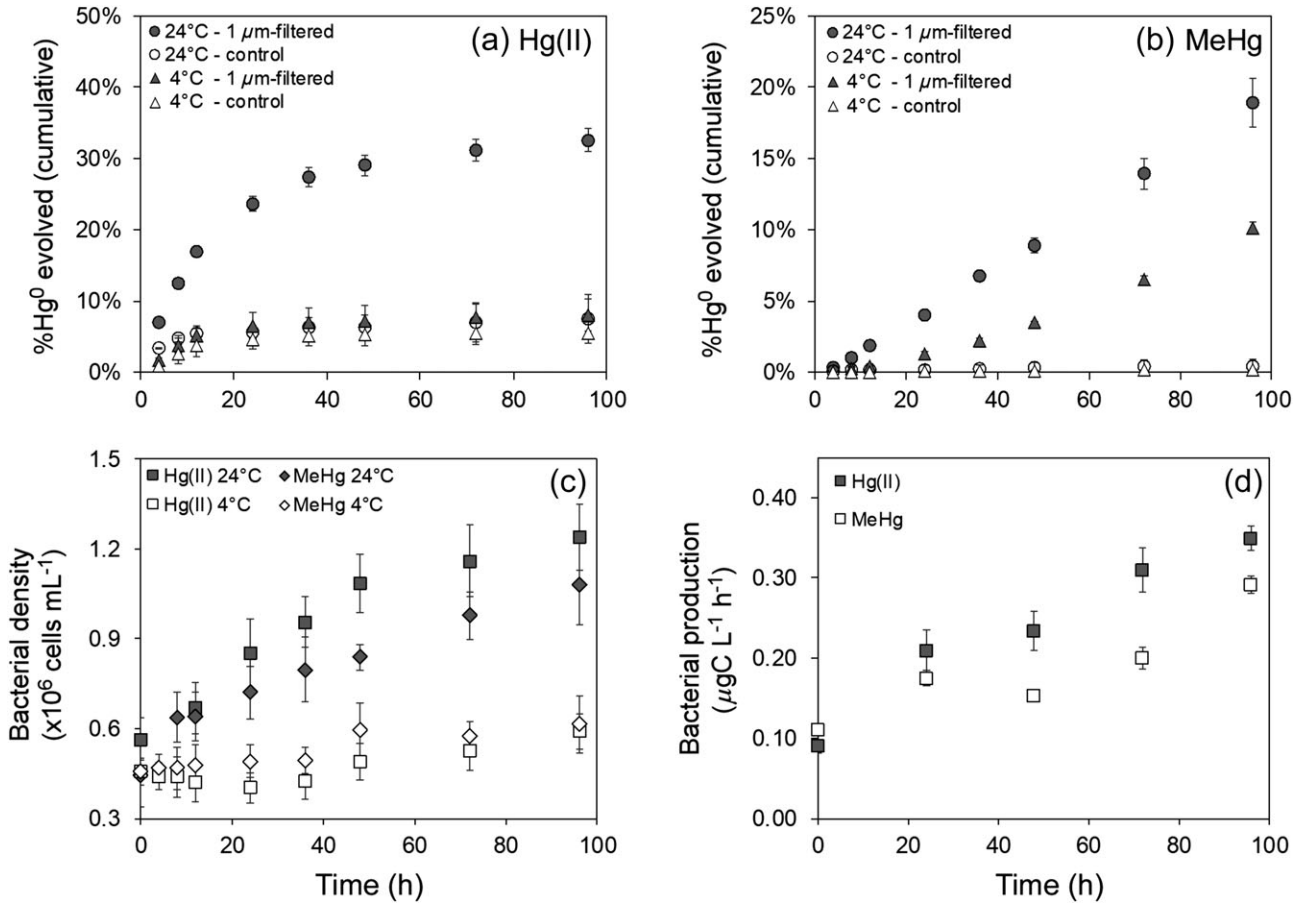

Fig. 4. Total percentage of Hg^0 evolved from (**a**) Hg(II)-treated SSW and (**b**) MeHg-treated SSW at two different temperatures, (**c**) microbial cell density, and (**d**) microbial production (24°C only) over time. Treatments with bacteria were 1 μm-filtered and controls were 0.2 μm sterile-filtered. Data points are the means from three replicate cultures with error bars of one standard deviation. Added concentrations of Hg(II) were 56 pM and of MeHg were 55 pM.

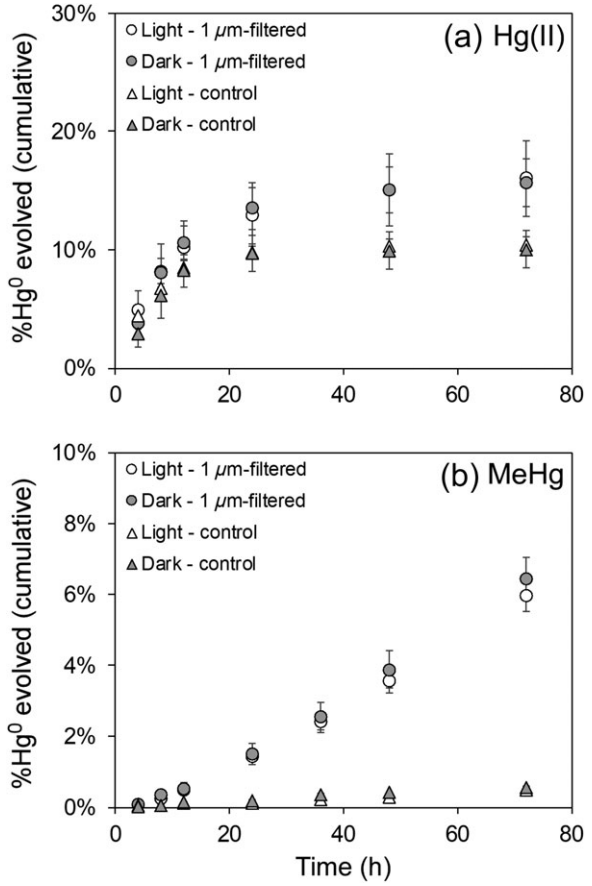

Fig. 5. Total percentage of Hg^0 evolved from (a) Hg(II)-treated SSW and (b) MeHg-treated SSW under light and dark conditions. Controls were sterile-filtered (0.2 μm) SSW. Data points are the means from two replicate cultures with error bars of one standard deviation. Added concentrations of Hg(II) were 45 pM and of MeHg were 70 pM.

Hg^0 production in freshly collected Long Island Sound seawater

The results of Hg^0 evolved from freshly collected LIW are shown in Fig. 6 (note that presented data contain unfiltered and 1 μm-filtered LIW). For Hg(II)-treated LIW, 70.5% ± 5.4%, 53.4% ± 3.1%, and 11.2% ± 1.3% of Hg^0 evolved from $LIW_{unfiltered}$, $LIW_{1\mu m}$, and LIW_{ctrl} after 96 h, respectively (Fig. 6a). For MeHg-treated LIW, 18.8% ± 0.6%, 7.9% ± 0.2%, and 0.4% ± 0.1% of Hg^0 evolved from $LIW_{unfiltered}$, $LIW_{1\mu m}$, and LIW_{ctrl} after 96 h, respectively (Fig. 6b). Microbial densities in LIW ranged from 4.3×10^6 cells mL^{-1} to 7.1×10^6 cells mL^{-1} (Fig. 6c).

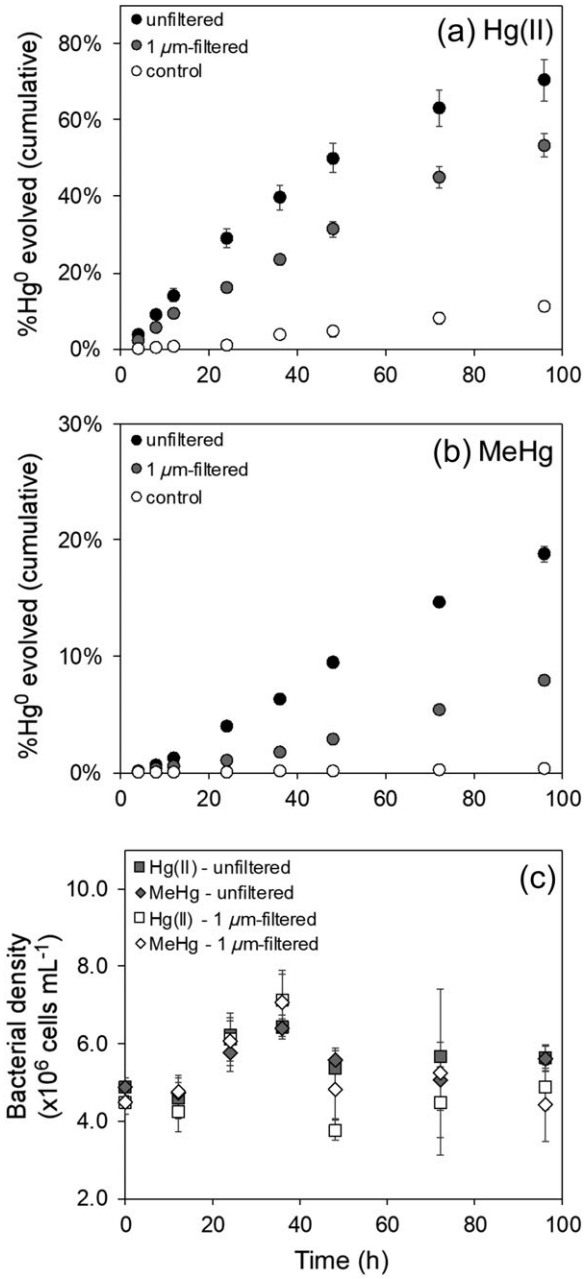

Fig. 6. Total percentage of Hg^0 evolved from (**a**) Hg(II)-treated LIW and (**b**) MeHg-treated LIW, and (**c**) microbial cell density at 24°C over time. Data points are the means from two replicate cultures with error bars of one standard deviation; error bars are often too small to see. Added concentrations of Hg(II) were 74 pM and of MeHg were 67 pM. Controls were sterile-filtered (0.2 μm) LIW.

Hg^0 production rate

After correcting for abiotic Hg^0 production in controls, average Hg^0 formation rates by bacteria in different treatments over 4 d of incubation are presented in Table 1. The Hg^0 production rates by bacteria at different time intervals were also calculated (Fig. 7a,b, data from $LIW_{unfiltered}$ not shown). For Hg(II)-treated seawater, the production rate was high at the first day (0–24 h) and then declined afterward (Fig. 7a). Notably, a significant decline after 1 d can be found in SSW (both 24°C and 4°C treatments). In contrast, a significant decline can be found after 3 d in LIW. For MeHg-treated seawater, the production rate gradually increased over time (Fig. 7b). The calculated Hg^0 production rate in Fig. 7a,b could have been biased by differences in the microbial biomass among

Table 1. Production of Hg^0 by marine bacteria in SSW and LIW in 4-d incubation experiments. All production rates from treatments with bacteria are corrected for abiotic production (controls, 0.2 μm sterile-filtered). Mean bacterial cell density represents the average bacterial density of all time points. In controls, bacterial cell densities were below detection limit (BDL).

Seawater type	Incubation temp. (°C)	Added Hg species	Total Hg^0 formation after 4 d (%)	Hg^0 formation (% d^{-1})	Mean bacterial density ($\times 10^6$ cells mL^{-1})	Hg^0 formation (% $d^{-1} \times 10^6$ $cells^{-1}$)	Hg^0 formation (amol-Hg d^{-1} $cells^{-1}$)	Rate constant ($\times 10^{-6}$ s^{-1})
$SSW_{1\mu m}$	24	Hg(II)	25.1 ± 1.2	6.3 ± 0.3	0.86 ± 0.10	7.3 ± 0.9	0.82 ± 0.10	1.1
$SSW_{1\mu m}$	24	MeHg	18.5 ± 1.7	4.6 ± 0.4	0.74 ± 0.09	6.2 ± 0.9	0.69 ± 0.11	0.61
SSW_{ctrl}	24	Hg(II)	7.6 ± 3.5	1.9 ± 0.9	BDL	—	—	0.14
SSW_{ctrl}	24	MeHg	0.5 ± 0.4	0.1 ± 0.1	BDL	—	—	< 0.01
$SSW_{1\mu m}$	4	Hg(II)	2.5 ± 2.7	0.6 ± 0.7	0.47 ± 0.07	1.3 ± 1.5	0.20 ± 0.22	0.06
$SSW_{1\mu m}$	4	MeHg	9.9 ± 0.4	2.5 ± 0.1	0.52 ± 0.11	4.8 ± 1.0	0.56 ± 0.12	0.30
SSW_{ctrl}	4	Hg(II)	5.6 ± 1.4	1.4 ± 0.4	BDL	—	—	0.17
SSW_{ctrl}	4	MeHg	0.2 ± 0.0	0.05 ± 0.01	BDL	—	—	< 0.01
$LIW_{1\mu m}$	24	Hg(II)	42.2 ± 3.1	10.5 ± 0.8	5.02 ± 0.58	2.1 ± 0.3	0.31 ± 0.04	1.3
$LIW_{1\mu m}$	24	MeHg	7.6 ± 0.2	1.9 ± 0.1	5.26 ± 0.83	0.4 ± 0.1	0.05 ± 0.01	0.17
$LIW_{unfiltered}$	24	Hg(II)	59.3 ± 5.4	14.8 ± 1.3	5.54 ± 0.39	2.7 ± 0.3	0.39 ± 0.05	2.2
$LIW_{unfiltered}$	24	MeHg	18.4 ± 0.6	4.6 ± 0.2	5.44 ± 0.38	0.8 ± 0.1	0.12 ± 0.01	0.47
LIW_{ctrl}	24	Hg(II)	11.2 ± 1.3	2.8 ± 0.3	BDL	—	—	0.27
LIW_{ctrl}	24	MeHg	0.4 ± 0.1	0.09 ± 0.03	BDL	—	—	< 0.01

treatments. Therefore, we further normalized the Hg^0 production rate to microbial density (Fig. 7c,d).

Discussion

Effects of Hg concentration and microbial densities

Regardless of the concentrations of dissolved Hg(II) or MeHg, the percentage of the total that resulted in Hg^0 formation in $SSW_{1\mu m}$ stayed constant over a 1-d incubation, suggesting that the fraction of total Hg that was bound to microbial cells remained constant and reached equilibrium rapidly across three concentrations. Limited by the specific activity of ^{203}Hg, the lowest Hg concentration used in this study was 1 pM, which was still higher than typical concentrations (fM to pM range) in nearly all marine ecosystems (especially for MeHg). Because there was no significant difference in Hg behavior across three concentrations (over 2 orders of magnitude), extrapolation of the experimental results to lower Hg concentrations may be valid.

Hg^0 production was positively correlated with microbial density, consistent with observations of Rolfhus and Fitzgerald (2004) in coastal seawater. Other studies demonstrated that Hg^0 production correlated with enzymatic activity (Barkay et al. 1991; Siciliano et al. 2002) and the biomass of planktonic organisms (Barkay et al. 1989; Mason et al. 1995), which also support the idea that biological activity contributes to Hg^0 production. The *y*-intercepts of the regression lines observed in Fig. 2b represent the percentage of abiotic Hg^0 formation in each treatment, ~9% for Hg(II) and ~1% for MeHg. These values are comparable to the results of background Hg gas formation described above in "Results" section.

Abiotic Hg^0 production from control treatments

The Hg^0 formation in SSW controls that were 0.2 μm sterile-filtered or autoclaved was consistent with findings that reactive Hg(II) might be reduced abiotically in a very short time in the presence of reductants in seawater or on flask walls (Mason et al. 1995). For controls of 0.2 μm-filtered SSW with antibiotics, no rapid Hg(II) reduction was observed in the first 24 h, which might be attributable to complexation of Hg(II) by the antibiotics, thereby inhibiting abiotic Hg(II) reduction. However, the effectiveness of antibiotics lasted only 1 d as Hg^0 formation increased up to 18% by 48 h, possibly due to degradation of antibiotics over time. No significant Hg^0 production was found among all MeHg-treated controls of SSW or LIW, suggesting that MeHg was very stable in seawater with respect to reduction without no bacteria and/or particles larger than 0.2 μm.

Effects of temperature and light

Nearly the same amount of Hg^0 was collected in controls between 24°C and 4°C, suggesting that continuous bubbling of air can sufficiently remove all produced Hg^0 from the dissolved phase and therefore the influence of changes in Hg^0 solubility due to varying temperatures was negligible. Note

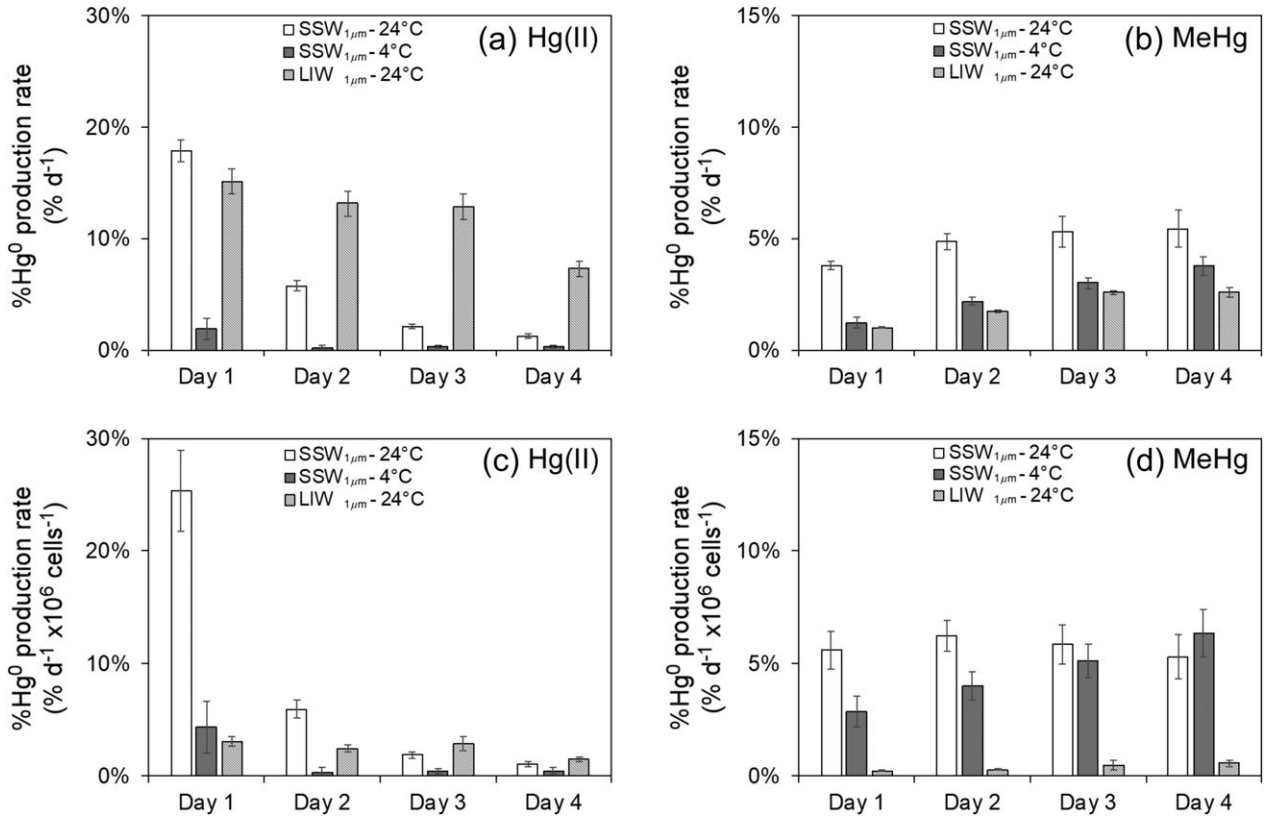

Fig. 7. Hg^0 production rate (corrected for controls) at different periods of time from (**a**) Hg(II)-treated seawater and (**b**) MeHg-treated seawater, and Hg^0 production rate (corrected for controls) normalized to microbial cell density from (**c**) Hg(II)-treated seawater and (**d**) MeHg-treated seawater. All data shown here were for 1 μm-filtered seawater and bars represent means of two or three replicate cultures with error bars of one standard deviation.

that this is within the normal annual range of water temperatures in Long Island waters. It was clear that more Hg^0 was produced at 24°C than at 4°C in either Hg(II)- or MeHg-treated $SSW_{1\mu m}$. For Hg(II) treatments, total $\%Hg^0$ production in $SSW_{1\mu m}$ was about four times higher at 24°C than at 4°C and the Q_{10} (calculated over the period 0–96 h) for the gas production rate process was 2.03 for Hg(II), consistent with a biologically mediated process. It is unlikely that abiotic reduction of Hg(II) occurring on microbial cell surfaces also contributed to the Hg gas production because Hg^0 formation in SSW_{ctrl} at 4°C was close to $SSW_{1\mu m}$ at 4°C where bacteria cells were present (Fig. 4a), suggesting that surface reduction only accounted for a small part of Hg^0 formation. In contrast, for MeHg-exposed cells, the Q_{10} of the Hg^0 production calculated over the first 96 h was only 1.11. The Q_{10} values calculated over the first 24 h for Hg(II) and MeHg were 2.09 and 1.38, respectively. There was a much sharper decline in Hg formation rates for Hg(II) than for MeHg after the first 24 h of exposure, expressed either on a whole culture basis or normalized to a microbial cell basis (Table 1).

The likeliest mechanism of Hg^0 formation from MeHg involves cleavage of the carbon-mercury bond by the organomercurial lyase, producing Hg(II), followed by the reduction of Hg(II) to Hg^0 by mercuric reductase (Ullrich et al. 2001). The Hg^0 production in MeHg-treated cultures at 4°C was similar to that of gross but greater than net production rates in Hg(II)-treated cultures at 4°C. Because gas formation in Hg(II)-treated seawater was much more influenced by temperature than in MeHg-treated seawater, it appears that the demethylation process might not be as sensitive to temperature as reduction of Hg(II) or, the gross demethylation process might be partially driven by an uncharacterized abiotic reaction which is not affected appreciably by temperature. Alternatively, abiotic MeHg degradation with thiols (Jonsson et al. 2016) and sulfides (Kanzler et al. 2018) to form DMHg has been shown to occur spontaneously. No sulfide was added in our treatments, but DMHg formation might be achieved if MeHg reacts with reduced sulfur groups on microbial cell surfaces. However, the tandem trap (Bond Elut ENV + gold beads) test showed that Hg^0 was the dominant species and the DMHg formation, if any, was negligible. The higher microbial production at 24°C than at 4°C, as inferred from leucine uptake, coincided with increased microbial cell densities over time. The measured values of microbial production were comparable to reports for natural assemblages of bacteria in field studies (Shiah and Ducklow 1994; Anderson and Taylor 2001).

Photochemical reactions through radiation of ultraviolet and visible light are known to reduce Hg(II) (Amyot

et al. 1994; Costa and Liss 2000; O'Driscoll et al. 2007) and degrade MeHg (Suda et al. 1993; Sellers et al. 1996; Hammerschmidt and Fitzgerald 2006; Lehnherr and St. Louis 2009; DiMento and Mason 2017), resulting in Hg^0 formation. However, we did not observe significant differences in Hg^0 evolution between light and dark treatments. The reason was probably due to our experimental settings where cool-white fluorescent light with very low ultraviolet radiation (Kritee et al. 2017) was used in our study. Moreover, its light intensity was less than one-twentieth of incident irradiation at full sunlight. Regardless of any light effects that may occur in nature, it was clear from the laboratory experiments that biologically mediated processes significantly enhanced the evasion of Hg from these cultures.

Unfiltered LIW vs. 1 μm-filtered LIW

Hg^0 production in Hg(II)-treated seawater was higher in $LIW_{unfiltered}$ than in $LIW_{1\mu m}$. Microbes smaller than 1 μm accounted for 71% of Hg(II) reduction in LIW, suggesting that these organisms are the primary Hg^0 producers, consistent with the conclusion of Mason et al. (1995). Hg^0 was also produced in MeHg-treated $LIW_{unfiltered}$ to a greater extent than in $LIW_{1\mu m}$, but microbes smaller than 1 μm only accounted for 41% of MeHg degradation. Whether this discrepancy is attributable to differential distribution of organomercurial lyase (MerB), the enzyme that is responsible for MeHg degradation, in different sized organisms is not known. In contrast, there appears to be broad distribution of the gene (*merA*) coding for mercuric reductase (MerA) which is responsible for Hg(II) reduction to gaseous Hg^0 and is the core enzyme of bacterial mercury resistance (Barkay et al. 2003).

Comparison of Hg^0 formation between SSW and LIW

The greater production of Hg^0 in Hg(II)-treated $LIW_{1\mu m}$ than in Hg(II)-treated $SSW_{1\mu m}$ was probably attributable to the greater microbial biomass in LIW. However, less Hg^0 production was found in MeHg-treated $LIW_{1\mu m}$ than in MeHg-treated $SSW_{1\mu m}$ which cannot be explained by differences in microbial biomass or other factors like salinity, dissolved organic matter, and nutrient concentrations. Further, the Hg^0 production in LIW was significantly lower than from SSW when normalized to microbial biomass. Assuming Hg^0 formation was mainly driven by microbial enzymatic processes, the discrepancy between SSW and LIW may have been a consequence of different microbial communities in these two waters, which in turn may have been partially attributable to the long storage of the SSW (6 yr) compared with the freshly collected LIW. Regardless, the rapid production of Hg^0 in SSW within 2 d of raising the temperature of this water from 4°C to 24°C was noteworthy.

The Hg-resistance gene, *merA*, is considered broadly distributed among bacteria and archaea probably due to horizontal gene transfer in evolution (Osborn et al. 1997; Boyd and Barkay 2012), but the prevalence of Hg-resistance among bacteria can vary from one location to another (Barkay et al. 2011). Further investigations using metagenomic analysis could elucidate the microbial community composition in SSW and LIW.

Bacterial mercuric reductase gene *merA*

There are two known MeHg degradation processes mediated by microbes, reductive demethylation by *merAB* yielding CH_4, and oxidative demethylation related to C1 metabolism in anaerobic prokaryotes yielding CO_2 and CH_4 (Barkay et al. 2003, 2011). Studies suggest that the reductive pathway is dependent on intracellular Hg concentrations (typically found in more heavily impacted environments) in more aerobic conditions, while the oxidative demethylation is more prevalent in anaerobic environments (Barkay et al. 2003; Hintelmann 2010; Grégoire and Poulain 2014). In addition, recent studies show a novel biological pathway of MeHg demethylation by methanotrophs but no production of gaseous Hg^0 is observed (Vorobev et al. 2013; Lu et al. 2017). Reductive demethylation is the likeliest process to have occurred in our experiments (assuming the demethylation was mediated by microbes), because the other processes are typically observed under low-redox conditions which did not occur in our experiments. As noted above, a new pathway of Hg(II) reduction has been observed for phototrophs that use Hg(II) as an electron sink to maintain intracellular redox homeostasis and generate Hg^0 (Grégoire and Poulain 2016), although this pathway has not yet been demonstrated for MeHg or specifically in heterotrophic bacterioplankton.

Following the procedure described by Poulain et al. (2015), *merA* genes in our positive control were successfully amplified at 300 bp (Supporting Information Fig. S1). Moreover, we found amplification of PCR product at ~300 bp (Supporting Information Fig. S1), which was used to determine presence of *merA* in our samples. The results suggest that the Hg^0 formation in our study may have been driven by bacterial mercuric reductase. It has been suggested that *merA*-mediated reduction is induced at high-ambient Hg(II) concentrations of > 50 pM (Morel et al. 1998); such a "threshold" concentration of Hg(II) is much higher than in most marine environments. Several field studies indeed showed detectable transcription of *mer* genes in highly contaminated environments (Nazaret et al. 1994; Schaefer et al. 2004). However, Poulain et al. (2007) reported detectable *merA* transcription in microbes in the Canadian Arctic where the ambient total Hg concentrations were about 10 pM, implying that bacteria may have continuous activity of Hg reductase even at natural, low Hg concentrations. Furthermore, they concluded that *merA*-mediated activity could account for up to 90% of Hg^0 production at a greater depth in the water column. In fact, *mer* induction should not only depend on absolute Hg concentrations but also other factors that affect actual Hg bioavailability to bacteria (Barkay et al. 2011). Our results showed that bacteria still exhibited significant capacity to produce Hg^0 at ambient

concentrations as low as ~5 pM. However, we did not determine if *merA* transcription was induced in our samples during the incubation. Further work is needed to elucidate whether threshold concentrations of Hg are applicable to bacteria.

Production kinetics and rates

Mason et al. (1995) examined Hg^0 formation in Hg(II)-treated seawater in diverse cultures of marine microorganisms (mostly phytoplankton, including cyanobacteria), and reported Hg^0 production rates of 0.4–9.7% d^{-1} (corresponding to 0.027–0.48 amol-Hg $cell^{-1}$ d^{-1}), which were comparable with our results (Table 1). However, it should be noted that their added Hg(II) concentrations were 0.5 nM which was about 10 times higher than ours. Monperrus et al. (2007) reported that microbial and/or phytoplanktonic reduction of Hg(II) in surface waters of the Mediterranean Sea ranged from 2.2% d^{-1} to 12.3% d^{-1}, which were also comparable to our study (Table 1).

The patterns of Hg^0 evolved from Hg(II)-treated seawater (initially rapid formation rates followed by much slower formation rates) were similar to the results from Barkay et al. (1991), where Hg(II) volatilization by an indigenous freshwater microbial community was measured. The decline in production rate in Hg(II) treatments was probably because of a decline in bioavailable Hg(II) for the bacteria and/or reactive Hg(II) was converted to a nonreducible form by complexation with dissolved organic matter. The Hg^0 production rates normalized to microbial abundance were significantly higher in SSW than in LIW, particularly within the first 48 h, possibly because the bacteria in SSW had a higher capacity to reduce Hg(II). The reaction of Hg(II) reduction from $SSW_{1\mu m}$ over 96 h seemed to be a mixed order reaction. But treated as a first order reaction, the calculated rate constant was 1.1×10^{-6} s^{-1}. The reaction for LIW can perfectly fit the model of a first order reaction and the rate constants were 1.3×10^{-6} s^{-1} for $LIW_{1\mu m}$ and 2.2×10^{-6} s^{-1} for $LIW_{unfiltered}$. These gross values are comparable to dark (or low light) gross values from incubations for the Baltic Sea ($1.5 \pm 0.5 \times 10^{-6}$ s^{-1}) (Kuss et al. 2015) and Chesapeake Bay and coastal shelf waters ($0.67–1.8 \times 10^{-6}$ s^{-1}) (Whalin et al. 2007), but rate constants of microbial production can be one to two orders of magnitude lower than those attributable to photochemical transformation at the ocean surface (O'Driscoll et al. 2006; Whalin et al. 2007; Qureshi et al. 2009; Vost et al. 2012).

Very few studies reported microbial MeHg demethylation rates and kinetics in seawater. Our calculated Hg^0 formation rates in MeHg-treated seawater (1.9–4.6% d^{-1}, Table 1) were comparable to Hg^0 production rates (2.8–10.9% d^{-1}) reported by Monperrus et al. (2007) in the Mediterranean. The Hg^0 evolved from MeHg-treated seawater was linear over time, implying a zero-order reaction with an independence of substrate (MeHg) concentrations. Unlike the Hg(II)-treated seawater, the Hg^0 formation rates in MeHg treatments did not change much over time. The modest increase over time is probably due to microbial growth over time as indicated by the low variability in Hg^0 production rate normalized to microbial densities. As noted earlier in the text, the formation of Hg^0 from MeHg is a likely two-step reaction involving the demethylation of MeHg to Hg(II), and the subsequent reduction to Hg^0. The demethylating process might be the rate limiting step, resulting in a linear increase of Hg^0 formation which was very different from the Hg(II)-treated seawater. In order to compare with Hg(II) treatments and previous literature, here we also used first order kinetics to calculate the rate constants for Hg^0 formation in MeHg-treated seawater. The calculated values were 0.61×10^{-6} s^{-1} for $SSW_{1\mu m}$, 0.17×10^{-6} s^{-1} for $LIW_{1\mu m}$, and 0.47×10^{-6} s^{-1} for $LIW_{unfiltered}$. Whalin et al. (2007) reported that the rate constants of demethylation in the water column of Chesapeake Bay were $< 1–5 \times 10^{-6}$ s^{-1} where the demethylation was driven by both photochemical and microbial processes. In a lab study using coastal seawater, rate constants attributable solely to photochemistry were reported to range from 10×10^{-6} s^{-1} to 19×10^{-6} s^{-1} (DiMento and Mason 2017). DiMento and Mason (2017) also demonstrated that photodegradation of MeHg decreases exponentially with depth, with degradation rates being < 10% of those in surface waters at depths < 5 m in estuaries, and 60 m in open ocean waters. Thus, biologically mediated conversion of MeHg would be expected to be greater than photochemical degradation of MeHg in subsurface waters, the absolute depth depending on light penetration in different water columns.

The distribution of Hg species in microbial cells may influence the kinetics of Hg(II) reduction and MeHg degradation. It has been shown that more MeHg can penetrate into the cytoplasm of phytoplankton cells than Hg(II) (Mason et al. 1996; Pickhardt and Fisher 2007; Lee and Fisher 2016). If this is also applicable to bacteria, rapid accumulation of MeHg into bacterial cytoplasm may therefore provide enough substrate (MeHg) to induce demethylation by the organomercurial lyase, resulting in continuous Hg^0 formation. In contrast, only part of the Hg(II) (free ion or neutral species) may be allowed to enter bacterial cells in the beginning of incubations and be reduced by mercuric reductase. Hu et al. (2013) reported that adsorption of Hg(II) by bacterial cells (*Geobacter sulfurreducens* PCA) would compete with, and therefore inhibit Hg(II) reduction. They suggested that the inhibition can be attributed to bonding between Hg(II) and the thiol functional groups on cells. Bioavailability of Hg(II) to microorganisms may be lowered because of further complexation of Hg(II) with other ligands (Barkay et al. 1997; Ullrich et al. 2001; Hsu-Kim et al. 2013; Schartup et al. 2015), explaining why less Hg^0 production was observed at a later stage of incubation (Fig. 7). Although MeHg can also form strong complexes with ligands which decrease its bioavailability to microorganisms (Ndu et al. 2016), Hg(II) is more prone to form metal complexes than MeHg because of its greater formation

constant with ligands. Similar cases can be seen in previous studies regarding MeHg production by Hg-methylating bacteria, where the highest methylation rate can be found in the first few days (Hamdy and Noyes 1975; Compeau and Bartha 1984; Ullrich et al. 2001).

In natural waters, Hg^0 formation is a combination of photochemical and microbial processes. The importance and relative contribution of each process on total Hg^0 formation may vary from one place to another. Some studies concluded that photochemical reduction of Hg(II) was the dominant process; for instance, earlier studies suggested that sunlight-induced gaseous Hg^0 formation was the most important route in lake water (Amyot et al. 1994) and coastal seawater (Amyot et al. 1997). Rolfhus and Fitzgerald (2004) estimated that approximately 70% of bulk reduction was driven photochemically and 20% was by microbial mediation in coastal surface seawater from Long Island Sound. Whalin et al. (2007) also suggested that biotic processes were relatively unimportant to Hg(II) reduction in surface waters of the Chesapeake. Tsui et al. (2013) and Point et al. (2011) used stable Hg isotopes as a proxy and concluded that photodegradation of MeHg is predominant in stream and Arctic marine ecosystems, respectively; they did not determine Hg^0 production. Although the photochemical production of Hg^0 can be very efficient, it is limited to the daytime and at the ocean's surface. Rapid water column attenuation of sunlight with depth can diminish the importance of the photochemical process, especially in high-latitude regions. For example, Poulain et al. (2007) reported that at a depth of 10 m below the surface of the Arctic Ocean, up to 90% of Hg^0 was produced by microbial reduction of Hg(II) rather than photochemical reduction. Kuss et al. (2015) reported that microbial production of Hg^0 under low-light conditions in the Baltic accounted for ~40% of total Hg^0 production. If the microbial transformation of Hg^0 can occur at any depth, the biological reduction of Hg(II) should become a significant source to the total pool of Hg^0 in the water column. Our findings indicate that microbial activity can convert MeHg as well as Hg(II) to Hg^0 and under light conditions typically prevalent at water depths of > 10 m, can contribute significantly to Hg^0 production. The Hg^0 gas produced has the potential to be released to the atmosphere, as shown here, but the extent to which this occurs under prevailing oceanographic conditions remains to be determined.

References

Amyot, M., D. J. McQueen, G. Mierle, and D. R. S. Lean. 1994. Sunlight-induced formation of dissolved gaseous mercury in lake waters. Environ. Sci. Technol. **28**: 2366–2371. doi:10.1021/es00062a022

Amyot, M., G. A. Gill, and F. M. M. Morel. 1997. Production and loss of dissolved gaseous mercury in coastal seawater. Environ. Sci. Technol. **31**: 3606–3611. doi:10.1021/es9703685

Anderson, T. H., and G. T. Taylor. 2001. Nutrient pulses, plankton blooms, and seasonal hypoxia in western Long Island Sound. Estuaries **24**: 228–243. doi:10.2307/1352947

Barkay, T., C. Liebert, and M. Gillman. 1989. Environmental significance of the potential for *mer*(Tn21)-mediated reduction of Hg^{2+} to Hg^0 in natural waters. Appl. Environ. Microbiol. **55**: 1196–1202.

Barkay, T., R. R. Turner, A. VandenBrook, and C. Liebert. 1991. The relationships of Hg(II) volatilization from a freshwater pond to the abundance ofmer genes in the gene pool of the indigenous microbial community. Microb. Ecol. **21**: 151–161. doi:10.1007/BF02539150

Barkay, T., M. Gillman, and R. R. Turner. 1997. Effects of dissolved organic carbon and salinity on bioavailability of mercury. Appl. Environ. Microbiol. **63**: 4267–4271.

Barkay, T., S. M. Miller, and A. O. Summers. 2003. Bacterial mercury resistance from atoms to ecosystems. FEMS Microbiol. Rev. **27**: 355–384. doi:10.1016/S0168-6445(03)00046-9

Barkay, T., N. Kroer, and A. J. Poulain. 2011. Some like it cold: Microbial transformations of mercury in polar regions. Polar Res. **30**: 1–15. doi:10.3402/polar.v30i0.15469

Baya, P. A., J. L. Hollinsworth, and H. Hintelmann. 2013. Evaluation and optimization of solid adsorbents for the sampling of gaseous methylated mercury species. Anal. Chim. Acta **786**: 61–69. doi:10.1016/j.aca.2013.05.019

Ben-Bassat, D., and A. M. Mayer. 1977. Reduction of mercury chloride by *Chlorella*: Evidence for a reducing factor. Physiol. Plant. **40**: 157–162. doi:10.1111/j.1399-3054.1977.tb04049.x

Bergquist, B. A., and J. D. Blum. 2007. Mass-dependent and-independent fractionation of Hg isotopes by photoreduction in aquatic systems. Science **318**: 417–420. doi:10.1126/science.1148050

Bergquist, B. A., and J. D. Blum. 2009. The odds and evens of mercury isotopes: Applications of mass-dependent and mass-independent isotope fractionation. Elements **5**: 353–357. doi:10.2113/gselements.5.6.353

Boyd, E., and T. Barkay. 2012. The mercury resistance operon: From an origin in a geothermal environment to an efficient detoxification machine. Front. Microbiol. **3**: 349. doi:10.3389/fmicb.2012.00349

Compeau, G., and R. Bartha. 1984. Methylation and demethylation of mercury under controlled redox, pH and salinity conditions. Appl. Environ. Microbiol. **48**: 1203–1207.

Costa, M., and P. S. Liss. 1999. Photoreduction of mercury in sea water and its possible implications for Hg^0 air–sea fluxes. Mar. Chem. **68**: 87–95. doi:10.1016/S0304-4203(99)00067-5

Costa, M., and P. S. Liss. 2000. Photoreduction and evolution of mercury from seawater. Sci. Total Environ. **261**: 125–135. doi:10.1016/S0048-9697(00)00631-8

DiMento, B. P., and R. P. Mason. 2017. Factors controlling the photochemical degradation of methylmercury in coastal

and oceanic waters. Mar. Chem. **196**: 116–125. doi:10.1016/j.marchem.2017.08.006

Fitzgerald, W. F., and G. A. Gill. 1979. Subnanogram determination of mercury by two-stage gold amalgamation and gas phase detection applied to atmospheric analysis. Anal. Chem. **51**: 1714–1720. doi:10.1021/ac50047a030

Fitzgerald, W. F., G. A. Gill, and J. P. Kim. 1984. An equatorial Pacific Ocean source of atmospheric mercury. Science **224**: 597–600. doi:10.1126/science.224.4649.597

Fitzgerald, W. F., C. H. Lamborg, and C. R. Hammerschmidt. 2007. Marine biogeochemical cycling of mercury. Chem. Rev. **107**: 641–662. doi:10.1021/cr050353m

Gionfriddo, C. M., and others. 2016. Microbial mercury methylation in Antarctic Sea ice. Nat. Microbiol. **1**: 16127. doi:10.1038/NMICROBIOL.2016.127

Grégoire, D. S., and A. J. Poulain. 2014. A little bit of light goes a long way: The role of phototrophs on mercury cycling. Metallomics **6**: 396–407. doi:10.1039/c3mt00312d

Grégoire, D. S., and A. . J. Poulain. 2016. A physiological role for Hg^{II} during phototrophic growth. Nat. Geosci. **9**: 121. doi:10.1038/ngeo2629

Hamdy, M. K., and O. R. Noyes. 1975. Formation of methyl mercury by bacteria. Appl. Microbiol. **30**: 424–432.

Hammerschmidt, C. R., and W. F. Fitzgerald. 2006. Photodecomposition of methylmercury in an arctic Alaskan lake. Environ. Sci. Technol. **40**: 1212–1216. doi:10.1021/es0513234

Hintelmann, H. 2010. Organomercurials. Their formation and pathways in the environment, p. 365–401. *In* A. Sigel, H. Sigel, and R. K. O. Sigel [eds.], Organometallics in environment and toxicology: Metal ions in life sciences. Royal Society of Chemistry.

Hsu-Kim, H., K. H. Kucharzyk, T. Zhang, and M. A. Deshusses. 2013. Mechanisms regulating mercury bioavailability for methylating microorganisms in the aquatic environment: A critical review. Environ. Sci. Technol. **47**: 2441–2456. doi:10.1021/es304370g

Hu, H., and others. 2013. Mercury reduction and cell-surface adsorption by *Geobacter sulfurreducens* PCA. Environ. Sci. Technol. **47**: 10922–10930. doi:10.1021/es400527m

Jonsson, S., N. M. Mazrui, and R. P. Mason. 2016. Dimethylmercury formation mediated by inorganic and organic reduced sulfur surfaces. Sci. Rep. **6**: 27958. doi:10.1038/srep27958

Kanzler, C. R., P. Lian, E. L. Trainer, X. Yang, N. Govind, J. M. Parks, and A. M. Graham. 2018. Emerging investigator series: Methylmercury speciation and dimethylmercury production in sulfidic solutions. Environ. Sci. Process. Impacts **20**: 584–594. doi:10.1039/C7EM00533D

Kim, J. P., and W. F. Fitzgerald. 1986. Sea-air partitioning of mercury in the equatorial Pacific Ocean. Science **231**: 1131–1134. doi:10.1126/science.231.4742.1131

Kirchman, D. L. 1993. Leucine incorporation as a measure of biomass production by heterotrophic bacteria, p. 509–512. *In* P. F. Kemp, B. F. Sherr, E. B. Sherr, and J. J. Cole [eds.], Handbook of methods in aquatic microbial ecology. CRC Press.

Kritee, K., J. D. Blum, M. W. Johnson, B. A. Bergquist, and T. Barkay. 2007. Mercury stable isotope fractionation during reduction of Hg(II) to Hg(0) by mercury resistant microorganisms. Environ. Sci. Technol. **41**: 1889–1895. doi:10.1021/es062019t

Kritee, K., J. D. Blum, and T. Barkay. 2008. Mercury stable isotope fractionation during reduction of Hg(II) by different microbial pathways. Environ. Sci. Technol. **42**: 9171–9177. doi:10.1021/es801591k

Kritee, K., T. Barkay, and J. D. Blum. 2009. Mass dependent stable isotope fractionation of mercury during *mer* mediated microbial degradation of monomethylmercury. Geochim. Cosmochim. Acta **73**: 1285–1296. doi:10.1016/j.gca.2008.11.038

Kritee, K., L. C. Motta, J. D. Blum, M. T.-K. Tsui, and J. R. Reinfelder. 2017. Photomicrobial visible light-induced magnetic mass independent fractionation of mercury in a marine microalga. ACS Earth Space Chem. **2**: 432–440. doi:10.1021/acsearthspacechem.7b00056

Kuss, J., N. Wasmund, G. N. Nausch, and M. Labrenz. 2015. Mercury emission by the Baltic Sea: A consequence of cyanobacterial activity, photochemistry, and low-light mercury transformation. Environ. Sci. Technol. **49**: 11449–11457. doi:10.1021/acs.est.5b02204

Lawson, N. M., and R. P. Mason. 1998. Accumulation of mercury in estuarine food chains. Biogeochemistry **40**: 235–247. doi:10.1023/A:1005959211768

Lee, C.-S., and N. S. Fisher. 2016. Methylmercury uptake by diverse marine phytoplankton. Limnol. Oceanogr. **61**: 1626–1639. doi:10.1002/lno.10318

Lee, C.-S., and N. S. Fisher. 2017. Bioaccumulation of methylmercury in a marine copepod. Environ. Toxicol. Chem. **36**: 1287–1293. doi:10.1002/etc.3660

Lee, S., and J. A. Fuhrman. 1987. Relationships between biovolume and biomass of naturally derived marine bacterioplankton. Appl. Environ. Microbiol. **53**: 1298–1303.

Lehnherr, I., and V. L. St. Louis. 2009. Importance of ultraviolet radiation in the photodemethylation of methylmercury in freshwater ecosystems. Environ. Sci. Technol. **43**: 5692–5698. doi:10.1021/es9002923

Lloyd, N. A., S. E. Janssen, J. R. Reinfelder, and T. Barkay. 2016. Co-selection of mercury and multiple antibiotic resistances in bacteria exposed to mercury in the *Fundulus heteroclitus* gut microbiome. Curr. Microbiol. **73**: 834–842. doi:10.1007/s00284-016-1133-6

Lu, X., W. Gu, L. Zhao, M. Farhan Ul Haque, D. S. AA, J. D. Semrau, and B. Gu. 2017. Methylmercury uptake and degradation by methanotrophs. Sci. Adv. **3**: e1700041.

Mason, R. P., and W. F. Fitzgerald. 1993. The distribution and biogeochemical cycling of mercury in the equatorial Pacific Ocean. Deep-Sea Res. Part I Oceanogr. Res. Pap. **40**: 1897–1924. doi:10.1016/0967-0637(93)90037-4

Mason, R. P., W. F. Fitzgerald, and F. M. M. Morel. 1994. The biogeochemical cycling of elemental mercury: Anthropogenic influences. Geochim. Cosmochim. Acta **58**: 3191–3198. doi:10.1016/0016-7037(94)90046-9

Mason, R. P., F. M. M. Morel, and H. F. Hemond. 1995. The role of microorganisms in elemental mercury formation in natural waters. Water Air Soil Pollut. **80**: 775–787. doi:10.1007/BF01189729

Mason, R. P., J. R. Reinfelder, and F. M. M. Morel. 1996. Uptake, toxicity, and trophic transfer of mercury in a coastal diatom. Environ. Sci. Technol. **30**: 1835–1845. doi:10.1021/es950373d

Mason, R. P., and G.-R. Sheu. 2002. Role of the ocean in the global mercury cycle. Global Biogeochem. Cycles **16**: 40.1–40.14. doi:10.1029/2001GB001440

Monperrus, M., E. Tessier, D. Amouroux, A. Leynaert, P. Huonnic, and O. F. X. Donard. 2007. Mercury methylation, demethylation and reduction rates in coastal and marine surface waters of the Mediterranean Sea. Mar. Chem. **107**: 49–63. doi:10.1016/j.marchem.2007.01.018

Morel, F. M. M., A. M. L. Kraepiel, and M. Amyot. 1998. The chemical cycle and bioaccumulation of mercury. Annu. Rev. Ecol. Syst. **29**: 543–566. doi:10.1146/annurev.ecolsys.29.1.543

Munson, K. M., D. Babi, and C. H. Lamborg. 2014. Determination of monomethylmercury from seawater with ascorbic acid-assisted direct ethylation. Limnol. Oceanogr.: Methods **12**: 1–9. doi:10.4319/lom.2014.12.1

Nazaret, S., W. H. Jeffrey, E. Saouter, R. Von Haven, and T. Barkay. 1994. *merA* gene expression in aquatic environments measured by mRNA production and Hg(II) volatilization. Appl. Environ. Microbiol. **60**: 4059–4065.

Ndu, U., T. Barkay, A. T. Schartup, R. P. Mason, and J. R. Reinfelder. 2016. The effect of aqueous speciation and cellular ligand binding on the biotransformation and bioavailability of methylmercury in mercury-resistant bacteria. Biodegradation **27**: 29–36. doi:10.1007/s10532-015-9752-3

Nriagu, J. O. 1994. Mechanistic steps in the photoreduction of mercury in natural waters. Sci. Total Environ. **154**: 1–8. doi:10.1016/0048-9697(94)90608-4

O'Driscoll, N. J., S. D. Siciliano, D. R. S. Lean, and M. Amyot. 2006. Gross photoreduction kinetics of mercury in temperate freshwater lakes and rivers: Application to a general model of DGM dynamics. Environ. Sci. Technol. **40**: 837–843. doi:10.1021/es051062y

O'Driscoll, N. J., L. Poissant, J. Canario, J. Ridal, and D. R. S. Lean. 2007. Continuous analysis of dissolved gaseous mercury and mercury volatilization in the upper St. Lawrence River: Exploring temporal relationships and UV attenuation. Environ. Sci. Technol. **41**: 5342–5348. doi:10.1021/es070147r

Oremland, R. S., C. W. Culbertson, and M. R. Winfrey. 1991. Methylmercury decomposition in sediments and bacterial cultures: Involvement of methanogens and sulfate reducers in oxidative demethylation. Appl. Environ. Microbiol. **57**: 130–137.

Osborn, A. M., K. D. Bruce, P. Strike, and D. A. Ritchie. 1997. Distribution, diversity and evolution of the bacterial mercury resistance (*mer*) operon. FEMS Microbiol. Rev. **19**: 239–262. doi:10.1111/j.1574-6976.1997.tb00300.x

Pickhardt, P. C., and N. S. Fisher. 2007. Accumulation of inorganic and methylmercury by freshwater phytoplankton in two contrasting water bodies. Environ. Sci. Technol. **41**: 125–131. doi:10.1021/es060966w

Point, D., and others. 2011. Methylmercury photodegradation influenced by sea-ice cover in Arctic marine ecosystems. Nat. Geosci. **4**: 188–194. doi:10.1038/ngeo1049

Poulain, A. J., and others. 2007. Potential for mercury reduction by microbes in the high arctic. Appl. Environ. Microbiol. **73**: 2230–2238. doi:10.1128/AEM.02701-06

Poulain, A. J., S. Aris-Brosou, J. M. Blais, M. Brazeau, W. B. Keller, and A. M. Paterson. 2015. Microbial DNA records historical delivery of anthropogenic mercury. ISME J. **9**: 2541. doi:10.1038/ismej.2015.86

Qureshi, A., N. J. O'Driscoll, M. MacLeod, Y.-M. Neuhold, and K. Hungerbühler. 2009. Photoreactions of mercury in surface ocean water: Gross reaction kinetics and possible pathways. Environ. Sci. Technol. **44**: 644–649. doi:10.1021/es9012728

Robinson, J. B., and O. H. Tuovinen. 1984. Mechanisms of microbial resistance and detoxification of mercury and organomercury compounds: Physiological, biochemical, and genetic analyses. Microbiol. Rev. **48**: 95.

Rolfhus, K. R., and W. F. Fitzgerald. 2001. The evasion and spatial/temporal distribution of mercury species in Long Island Sound, CT-NY. Geochim. Cosmochim. Acta **65**: 407–418. doi:10.1016/S0016-7037(00)00519-6

Rolfhus, K. R., and W. F. Fitzgerald. 2004. Mechanisms and temporal variability of dissolved gaseous mercury production in coastal seawater. Mar. Chem. **90**: 125–136. doi:10.1016/j.marchem.2004.03.012

Rouleau, C., and M. Block. 1997. Fast and high-yield synthesis of radioactive CH_3 ^{203}Hg (II). Appl. Organomet. Chem. **11**: 751–753. doi:10.1002/(SICI)1099-0739(199709)11:9<751::AID-AOC631>3.0.CO;2-Z

Schaefer, J. K., J. Yagi, J. R. Reinfelder, T. Cardona, K. M. Ellickson, S. Tel-Or, and T. Barkay. 2004. Role of the bacterial organomercury lyase (*merB*) in controlling methylmercury accumulation in mercury-contaminated natural waters. Environ. Sci. Technol. **38**: 4304–4311. doi:10.1021/es049895w

Schartup, A. T., U. Ndu, P. H. Balcom, R. P. Mason, and E. M. Sunderland. 2015. Contrasting effects of marine and terrestrially derived dissolved organic matter on mercury speciation and bioavailability in seawater. Environ. Sci. Technol. **49**: 5965–5972. doi:10.1021/es506274x

Sellers, P., C. A. Kelly, J. W. M. Rudd, and A. R. MacHutchon. 1996. Photodegradation of methylmercury in lakes. Nature **380**: 694. doi:10.1038/380694a0

Sherr, B., E. Sherr, and P. del Giorgio. 2001. Enumeration of total and highly active bacteria, p. 129–159. *In* J. H. Paul [ed.], Methods in microbiology. Academic Press.

Shiah, F.-K., and H. W. Ducklow. 1994. Temperature and substrate regulation of bacterial abundance, production and specific growth rate in Chesapeake Bay, USA. Mar. Ecol. Prog. Ser. **103**: 297–308. doi:10.3354/meps103297

Siciliano, S. D., N. J. O'Driscoll, and D. Lean. 2002. Microbial reduction and oxidation of mercury in freshwater lakes. Environ. Sci. Technol. **36**: 3064–3068. doi:10.1021/es010774v

Suda, I., M. Suda, and K. Hirayama. 1993. Degradation of methyl and ethyl mercury by singlet oxygen generated from sea water exposed to sunlight or ultraviolet light. Arch. Toxicol. **67**: 365–368. doi:10.1007/BF01973709

Tsui, M. T. K., J. D. Blum, J. C. Finlay, S. J. Balogh, S. Y. Kwon, and Y. H. Nollet. 2013. Photodegradation of methylmercury in stream ecosystems. Limnol. Oceanogr. **58**: 13–22. doi:10.4319/lo.2013.58.1.0013

Ullrich, S. M., T. W. Tanton, and S. A. Abdrashitova. 2001. Mercury in the aquatic environment: A review of factors affecting methylation. Crit. Rev. Environ. Sci. Technol. **31**: 241–293. doi:10.1080/20016491089226

Vetriani, C., Y. S. Chew, S. M. Miller, J. Yagi, J. Coombs, R. A. Lutz, and T. Barkay. 2005. Mercury adaptation among bacteria from a deep-sea hydrothermal vent. Appl. Environ. Microbiol. **71**: 220–226. doi:10.1128/AEM.71.1.220-226.2005

Vorobev, A., S. Jagadevan, B. S. Baral, A. A. Dispirito, B. C. Freemeier, B. H. Bergman, N. L. Bandow, and J. D. Semrau. 2013. Detoxification of mercury by methanobactin from *Methylosinus trichosporium* OB3b. Appl. Environ. Microbiol. **79**: 5918–5926. doi:10.1128/AEM.01673-13

Vost, E. E., M. Amyot, and N. J. O'Driscoll. 2012. Photoreactions of mercury in aquatic systems, p. 193–218. *In* G. Liu, Y. Cai, and N. J. O'Driscoll [eds.], Environmental chemistry and toxicology of mercury. Wiley.

Whalin, L., E.-H. Kim, and R. P. Mason. 2007. Factors influencing the oxidation, reduction, methylation and demethylation of mercury species in coastal waters. Mar. Chem. **107**: 278–294. doi:10.1016/j.marchem.2007.04.002

Yu, H., L. Chu, and T. K. Misra. 1996. Intracellular inducer Hg^{2+} concentration is rate determining for the expression of the mercury-resistance operon in cells. J. Bacteriol. **178**: 2712–2714. doi:10.1128/jb.178.9.2712-2714.1996

Zheng, W., and H. Hintelmann. 2009. Mercury isotope fractionation during photoreduction in natural water is controlled by its Hg/DOC ratio. Geochim. Cosmochim. Acta **73**: 6704–6715. doi:10.1016/j.gca.2009.08.016

Acknowledgments

We thank J. Reinfelder and R. Mason for access to some instrumentation and helpful comments and Z. Baumann, B. Dimento, N. Lloyd, S. Crane, A. Cohen, G. Taylor, and C.-L. Lin for technical assistance. We also thank two anonymous reviewers for constructive comments. This research was supported by NSF Awards PLR1260345 and OCE1634024, NIEHS Award P42ES007373, and the Gelfond Fund for Mercury Research.

Conflict of Interest

None declared.

Submitted 02 July 2018
Revised 01 September 2018
Accepted 05 October 2018

Associate editor: Luiz Drude de Lacerda